

07.2;07.3

Spreading resistance microscopy for determination of the barrier layer parameters in nBn structures based on InSb

© K.A. Savin¹, A.V. Klekovkin¹, I.I. Minaev¹, G.N. Eroshenko¹, V.S. Krivobok^{1,2},
D.E. Sviridov¹, A.E. Goncharov², S.N. Nikolaev¹

¹ Lebedev Physical Institute, Russian Academy of Sciences, Moscow, Russia

² Orion R&P Assoc, Moscow, Russia

E-mail: savinkonstantin93@gmail.com

Received May 8, 2024

Revised May 8, 2024

Accepted June 7, 2024

A new approach is demonstrated that allows visualization of the electronic subsystem of InSb/InAlSb barrier-diode structures, evaluation of the homogeneity of the InAlSb layer that blocks majority carriers in such structures, and determination of the height of the corresponding potential barrier. The approach is based on measuring the spreading resistance on a freshly prepared (110) cleaved cross-section of the epitaxial heterostructure with a diamond-coated silicon probe.

Keywords: current spreading resistance, molecular beam epitaxy, IR photodetector, InSb, barrier diode heterostructures.

DOI: 10.61011/TPL.2024.10.59690.19986

Indium antimonide (InSb) and solid solutions based on it are used widely in fabrication of mid-IR photodetectors [1,2]. At the same time, modern scholarship regards generation-recombination processes associated with the Shockley–Read–Hall mechanism as one of the most significant sources of noise in such detectors [3]. It is known that noise of this kind is suppressed by introducing a unipolar barrier blocking the majority carriers [4]. This is the reason why the development of techniques for epitaxial growth of nBn structures based on InSb is one of the relevant research trends in mid-IR photosensorics [5].

The advancement of techniques for epitaxial growth of heterostructures with a unipolar barrier needs to be coupled with the development of methods for monitoring their electrophysical properties, which involves primarily the analysis of homogeneity of the blocking layer and the determination of height of the corresponding potential barrier. These factors are crucial for a unipolar barrier IR detector, since its noise characteristics and capacity to operate at elevated temperatures depend largely on them. In the present study, InSb/InAlSb/InSb epitaxial structures with an InAlSb unipolar barrier are used as an example to demonstrate that mapping of the spreading resistance on a (110) heterostructure cleaved cross-section at room temperature is a simple and efficient method for unipolar barrier monitoring.

InSb-based nBn structures were grown by molecular beam epitaxy on *n*-type InSb (100) substrates using a Riber Compact-21T system. The barrier in these heterostructures was formed by an InAlSb layer with a thickness of ~ 70 nm. InSb layers with a thickness up to 400 nm doped with tellurium to 10^{17} cm⁻³ were used to form top and bottom contacts. The design of the structure is presented in Fig. 1, *a*. A typical AFM image of the surface of the obtained nBn

structure is shown in Fig. 1, *b*. There are no visible defects on the surface of samples; the average roughness is 0.24 nm, which is less than the thickness of a single monolayer and is indicative of atomic smoothness of the surface. The parameters of layers in the structures were verified by the results of measurements of X-ray rocking curves and their subsequent modeling (Fig. 1, *c*). Spreading resistance microscopy (SRM) measurements were carried out with a Solver P47 Pro (NT-MDT) scanning probe microscope at room temperature under atmospheric conditions. Silicon probes with a diamond conductive coating doped with boron (DCP30) were used. The contact force was ~ 1000 nN. The second contact was established by applying liquid InGa eutectic to a freshly cleaved surface. A dc bias was applied to this contact, and the probe was grounded.

Figure 2, *a* shows the typical two-dimensional map of spreading resistance for the nBn architecture obtained at a voltage of $U = -4$ mV. For clarity, the averaged dependence of current on the tip position on the cleaved cross-section in the growth direction is shown in Fig. 2, *b*. The expected contrast in the barrier region and differences in current between the contact and absorber layers (attributable to the difference in doping levels) are evident in Fig. 2, *b*. The design thicknesses match those determined based on the data from Fig. 2, *a*. At the same time, effects associated with barrier shorting due to potential material segregation in the course of epitaxial growth are lacking.

Figure 2, *c* shows the current–voltage curves obtained in different regions of the heterostructure. The observed linearity is indicative of ohmic nature of the tip–semiconductor contact. The current signal is determined as $I = U/R_{total}$, and R_{total} is the sum of probe resistance R_p and spreading resistance R_s of the examined sample. The presence of the contrast from layers with different conductivity

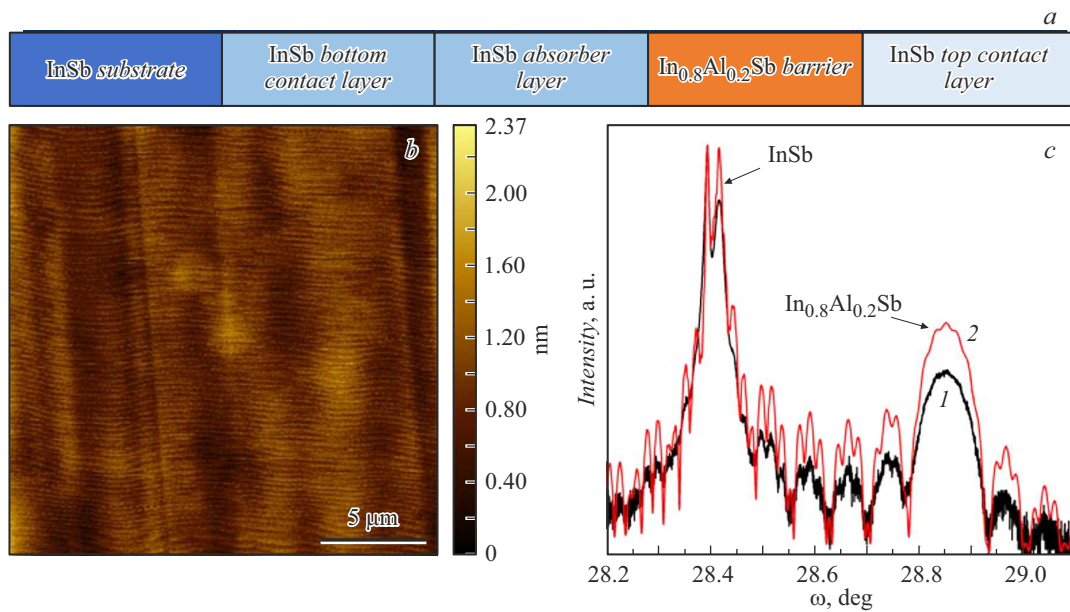


Figure 1. *a* — Design of the InSb-based nBn structure; *b* — AFM image of the structure surface; *c* — XRD image of the structure (*1* — experimental data; *2* — calculation for the structure with an $\text{In}_{0.8}\text{Al}_{0.2}\text{Sb}$ barrier 66 nm in thickness).

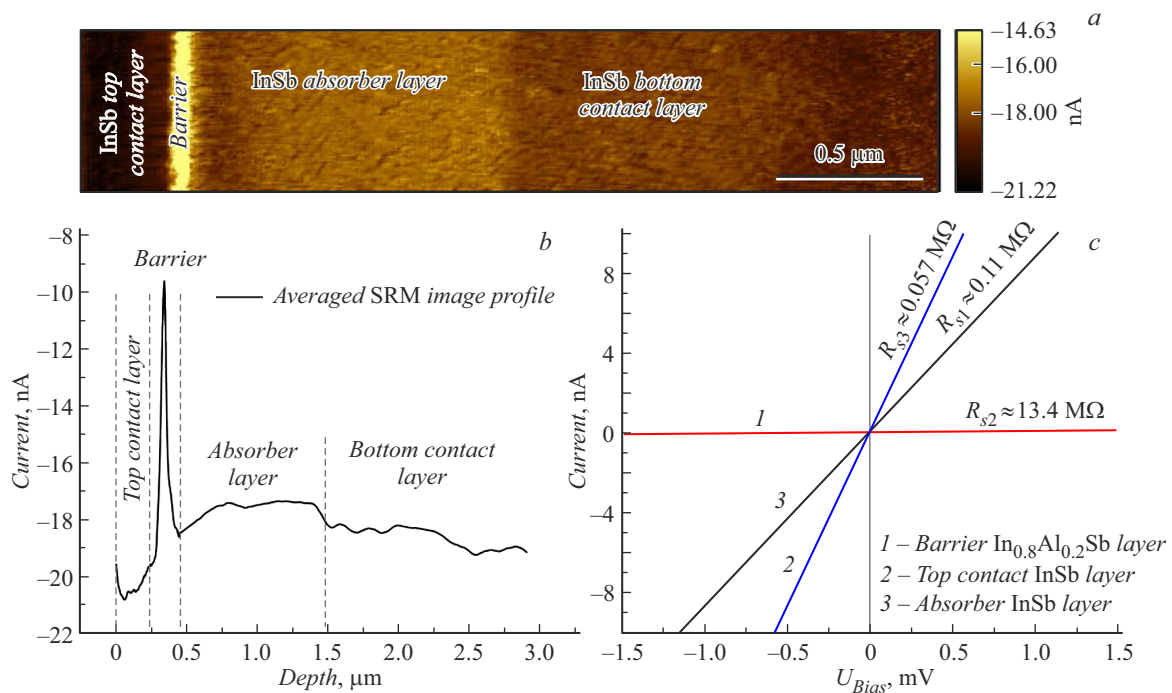


Figure 2. *a* — Two-dimensional SRM signal map for the InSb/InAlSb nBn structure obtained at $U = -4$ mV; *b* — averaged profile of the two-dimensional map; *c* — current-voltage curves obtained in different regions of the structure under the same conditions.

on the cleaved cross-section suggests that $R_s \gg R_p$ and, consequently, the probe resistance may be neglected in the conditions of our experiment: $I \approx U/R_s$.

The spreading resistance is specified by the density of carriers and their mobility. This implies that the ratio of current signals at two points allows one to determine the ratio of carrier densities if the ratio of mobilities is known: $I_1/I_2 \propto R_{s2}/R_{s1} \propto \sigma_1/\sigma_2 \propto n_1\mu_1/n_2\mu_2$. Since all

measurements were carried out at room temperature, the main factor governing the carrier mobility in the material is the optical phonon scattering corresponding to the In–Sb and Al–Sb bonds. Taking into account the low (20%) molar fraction of aluminum and the ratio of characteristic frequencies for LO phonons corresponding to different types of bonds [6,7] it is fair to say that the electron mobility in $\text{In}_{1-x}\text{Al}_x\text{Sb}$ ($x \approx 0.2$) should differ only slightly from

that for InSb in the experiment. Effective electron mass $m_{n2}^* = 0.05m_0$ in $\text{In}_{1-x}\text{Al}_x\text{Sb}$ ($x \approx 0.2$) may be taken from the linear dependence of the effective electron mass on the band gap for InSb and AlSb [8].

The above approximations allow one to use the SRM to estimate the unipolar barrier height in the system under consideration based on the standard expression for the density of charge carriers near the conduction band bottom:

$$n_{CB} = N_C \exp\left(-\frac{E_C - E_F}{kT}\right),$$

where

$$N_C = 2 \left(\frac{2\pi m_n^* kT}{h^2} \right)^{3/2}.$$

E_C is the energy of the conduction band bottom, and E_F is the chemical potential. In the presence of a detailed equilibrium between the absorbing InSb layer and the $\text{In}_{1-x}\text{Al}_x\text{Sb}$ barrier, the $E_{F1} = E_{F2}$ equality is satisfied. Thus, the following expression may be obtained for barrier height ΔE_C :

$$\Delta E_C = kT \ln \left[\frac{\sigma_1}{\sigma_2} \left(\frac{m_{n2}^*}{m_{n1}^*} \right)^{3/2} \right] = kT \ln \left[\frac{R_{s2}}{R_{s1}} \left(\frac{m_{n2}^*}{m_{n1}^*} \right)^{3/2} \right]. \quad (1)$$

Inserting the values of R_s derived from Fig. 2, *c* into (1), we find that barrier height ΔE_C in the conduction band is 0.18 eV. This result is consistent with the calculated data for $\text{In}_{1-x}\text{Al}_x\text{Sb}$ barrier layers presented in [5]. It should also be noted that mechanical stresses arising from the lattice mismatch between $\text{In}_{1-x}\text{Al}_x\text{Sb}$ ($x \approx 0.2$) and InSb reduce E_g [9], which, in turn, affects the height of ΔE_C ; however, further research is needed to perform a more detailed assessment of this contribution.

Thus, the electronic subsystem of InSb/InAlSb/InSb nBn structures obtained by molecular beam epitaxy was examined by spreading resistance microscopy. Measurements were performed on fresh cross-sections of heterostructures corresponding to the (110) plane. It was demonstrated that the probe resistance is insignificant even in the case of moderately doped layers when silicon probes with a diamond coating are used. Owing to this, spreading resistance microscopy may be viewed as a method for direct mapping of the product of density of majority carriers and their mobility. Since the electron mobility in materials of this group is known, one may convert the signal into carrier density and then reconstruct the potential profile in the conduction band. Thus, spreading resistance microscopy provided an opportunity not only to visualize the inhomogeneity of the electronic subsystem associated with blocking InAlSb layers, but also to estimate the height of the corresponding potential barrier. Therefore, spreading resistance microscopy may well be regarded as an efficient method for characterization of nBn structures that are used to produce multichannel mid-IR detectors.

Funding

This study was supported financially by the Russian Science Foundation as part of project No. 19-79-30086.

Conflict of interest

The authors declare that they have no conflict of interest.

References

- [1] H. Heidarzaden, Phys. Status Solidi B, **260** (3), 2200358 (2022). DOI: 10.1002/pssb.202200358
- [2] M.A. Sukhanov, A.K. Bakarov, D.Yu. Protasov, K.S. Zhuravlev, Tech. Phys. Lett., **46**, 154 (2020). DOI: 10.1134/S1063785020020285.
- [3] F.M. Klaassen, J. Blok, F.J. De Hoog, Physica, **27** (2), 185 (1961). DOI: 10.1016/0031-8914(61)90041-6
- [4] S. Maimon, G.W. Wicks, Appl. Phys. Lett., **89** (15), 151109 (2006). DOI: 10.1063/1.2360235
- [5] A. Evirgen, J. Abautret, J.P. Perez, A. Cordat, A. Nedelcu, P. Christol, Electron. Lett., **50** (20), 1472 (2014). DOI: 10.1049/el.2014.2799
- [6] R. Xiao, H. Yan, Y. Pei, B. Li, K. Yang, J. Liu, X. Liu, J. Mater. Sci.: Mater. Electron., **30** (14), 13290 (2019). DOI: 10.1007/s10854-019-01692-4
- [7] H. Liu, Y. Zhang, E.H. Steenbergen, S. Liu, Z. Lin, Y.-H. Zhang, J. Kim, M.-H. Ji, T. Detchprohm, R.D. Dupuis, J.K. Kim, S.D. Hawkins, J.F. Klem, Phys. Rev. Appl., **8** (3), 034028 (2017). DOI: 10.1103/PhysRevApplied.8.034028
- [8] J. Singh, *Semiconductor devices: basic principles* (John Wiley & Sons, 2000).
- [9] Y. Sun, S.E. Thompson, T. Nishida, J. Appl. Phys., **101** (10), 104503 (2007). DOI: 10.1063/1.2730561

Translated by D.Safin